FCIC pyrolysis modeling

Gavin Wiggins
wigginsg@ornl.gov

September 16, 2021

Contents

1 Introduction

This report discusses biomass pyrolysis fluidized bed reactor modeling activities for the Feedstock-Conversion Interface Consortium (FCIC) project. Model parameters are based on the NREL 2FBR biomass fast pyrolysis system which is comprised of a two-inch diameter bubbling fluidized bed (BFB) reactor. Experiment data, apparatus information, and material data are provided by the National Renewable Energy Laboratory (NREL), the National Energy Technology Laboratory (NETL), and the Idaho National Laboratory (INL). Model development and associated results are provided by Oak Ridge National Laboratory (ORNL).

2 Experimental apparatus and data

Information about the fluidized bed reactor such as typical operating conditions and reactor geometry is provided in this section. Data pertaining to proximate and ultimate analysis, chemical analysis, and particle characteristics for each feedstock are also presented. Characteristics of the bed particles are also provided. Lastly, measured product yields from the fast pyrolysis of each feedstock are given in this section too.

2.1 Apparatus

The BFB pyrolysis reactor at NREL is operated at fast pyrolysis conditions to thermochemically convert biomass feedstock into gas, tar, and char products. Pyrolysis occurs in a fluidized bed reactor comprised of a bed of sand fluidized by nitrogen gas. Biomass particles are fed into the bed via an auger and secondary gas stream at the side of the reactor. An overview of the components and flows related to the pyrolysis reactor (pyrolyzer) is given in Figure 1. The diagram was created using information provided by NREL [4].

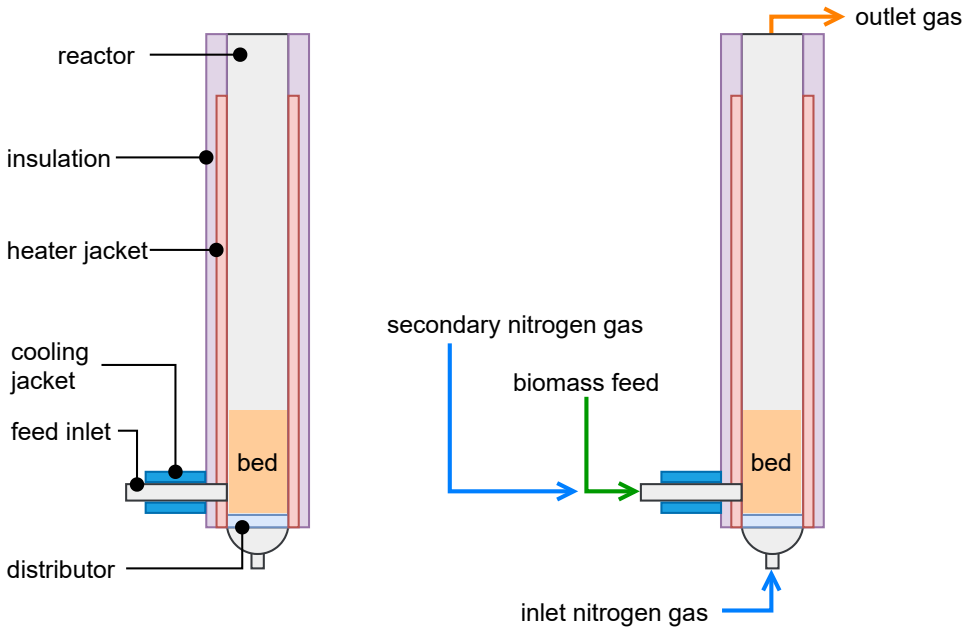

Figure 1: Components (left) and inlet/outlet flows (right) of the NREL bubbling fluidized bed pyrolysis reactor.

Dimensions for the reactor tube, feed inlet, insulation, heat jacket, and distributor plate are given in Figure 2 and Table 1. The main reactor tube is a 2-inch Schedule 40 pipe; therefore, the inner and outer reactor diameters are determined from nominal pipe size tables. The gas distributor contains 18 holes in a triangular pattern [4].

Typical operating conditions of the pyrolyzer are presented in Table 2. Pressure drop across the distributor is about 80-90 inches of H_2O. Nitrogen gas is used to fluidize the bed and assist biomass particles through the feed inlet tube. Experiments are conducted with an initial mass of sand in the bed; sand is not fed into the reactor during operation. Insulation surrounds the reactor while heat jackets extend almost the entire height of the unit. A cooling jacket surrounds the feed inlet tube. Pyrolysis vapors exit directly out the top of the reactor via a straight tube [4].

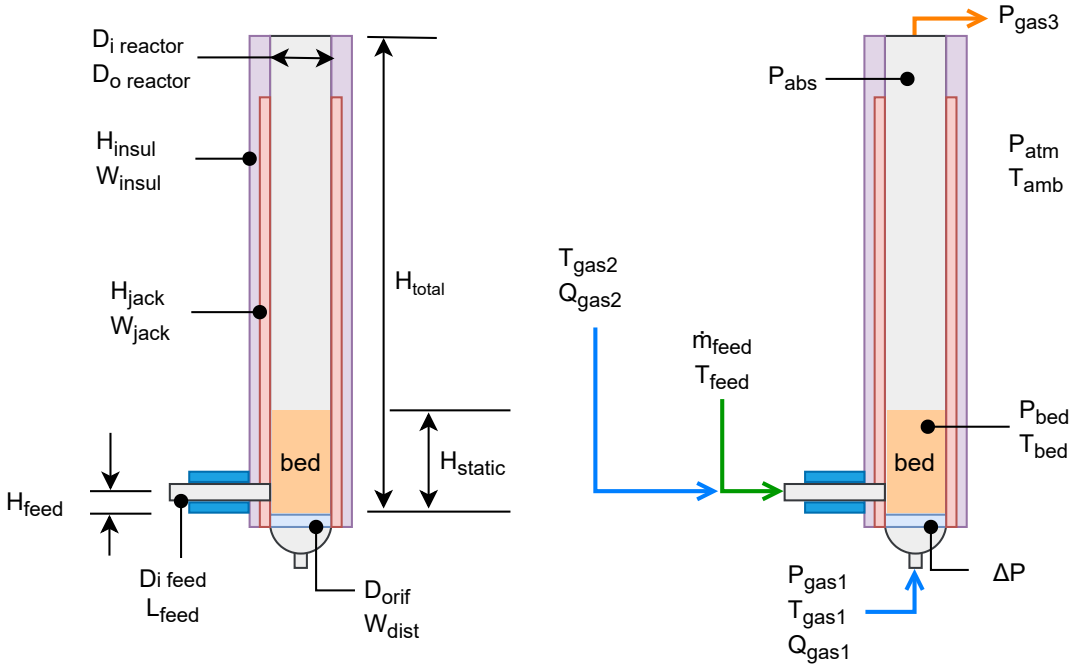

Figure 2: Dimensions and typical fast pyrolysis operating conditions for the NREL 2FBR pyrolyzer reactor.

Table 1: Dimensions for components of the fluidized bed pyrolysis reactor.

Reactor dimension	Symbol	Value	Units
Inner reactor diameter	$D_{i,\ reactor}$	5.25	cm
Outer reactor diameter	$D_{o,\ reactor}$	6.03	cm
Static bed height	H_{static}	10.16	cm
Total reactor height	H_{total}	43.18	cm
Feed inlet inner diameter	$D_{i,\ feed}$	1.27	cm
Feed height from top of distributor	H_{feed}	1.9	cm
Feed inlet tube length	L_{feed}	18.29	cm
Insulation height	H_{insul}	43.18	cm
Insulation thickness	W_{insul}	10	cm
Jacket height	H_{jack}	35	cm
Jacket thickness	W_{jack}	5	cm
Diameter of distributor orifices	D_{orif}	0.08	cm
Thickness of distributor plate	W_{dist}	3.17	mm
Number of orifices in distributor	n	18	–

Table 2: Typical operating conditions for the fluidized bed pyrolysis reactor. Atmospheric pressure considers elevation of NREL site in Golden, CO.

Reactor condition	Symbol	Value	Units
Absolute pressure in reactor	P_{abs}	101.3	kPa
Atmospheric pressure	P_{atm}	81	kPa
Ambient air temperature	T_{amb}	300.15	K
Absolute bed pressure	P_{bed}	115	kPa
Bed temperature	T_{bed}	773.15	K
Pressure drop over distributor	Δ P	21.17	KPa
Absolute inlet gas pressure	P_{gas1}	110–140	kPa
Inlet gas temperature	T_{gas1}	773.15	K
Inlet gas flowrate	Q_{gas1}	14	SLM (0.29 g/s)
Secondary gas temperature	T_{gas2}	298.15	K
Secondary gas flowrate	Q_{gas2}	1.4	SLM (0.029 g/s)
Absolute outlet gas pressure	P_{gas3}	90–110	kPa
Biomass inlet feedrate	$\dot{m}_{feed}$	420	g/hr
Biomass inlet temperature	T_{feed}	298.15	K

2.2 Feedstock proximate and ultimate analyses

Proximate and ultimate analysis measurements for each feedstock are given in Tables 3 and 4 on an as-determined basis (ad). A visual comparison of the proximate and ultimate analysis measurements is shown in Figure 3. Overall, the elemental composition of each feedstock is similar based on the ultimate analysis data. Differences in elemental fractions occur mainly in the C and O fractions with a maximum difference of approximately 3 wt.% and 5 wt.% respectively. For the proximate analysis fractions, the largest differences are observed for the fixed carbon (FC) and volatile matter (VM) at 10 wt.% and 13 wt.% respectively. A maximum difference of about 3 wt.% is seen for the ash and moisture fractions.

Table 3: Proximate analysis measurements given as wt. % as-determined basis.

Name	Cycle	FC	VM	Ash	Moisture	Total
Residues	1	20.72	72.92	1.45	4.92	100.01
Stem wood	2	16.79	79.40	0.28	3.55	100.02
Bark	3	27.16	66.29	0.70	5.86	100.01
Needles	4	23.26	69.54	3.78	3.42	100.00
Bark + needles	5	24.35	68.30	2.52	4.85	100.02
Residues (rep 1)	8	20.78	72.37	1.65	5.20	100.00
Residues:bark:needles 1:1:1	10	23.75	69.02	2.05	5.19	100.01
Residues:bark:needles 1:2:2	11	24.12	68.57	2.02	5.29	100.00
Air classified (10 Hz)	12	19.92	75.59	0.92	3.57	100.00
Air classified (28 Hz)	13	18.68	76.31	0.61	4.41	100.01
Whole tree (13 yr)	15	19.15	76.72	0.44	3.71	100.02
Stem wood (13 yr)	16	18.60	78.37	0.30	2.75	100.02
Maximum difference		10.37	13.11	3.50	3.11	

Table 4: Ultimate analysis measurements given as wt. % as-determined basis.

Name	Cycle	C	H	O	N	S	Total
Residues	1	49.63	6.52	41.87	0.49	0.04	98.55
Stem wood	2	48.89	6.53	44.12	0.18	0.01	99.73
Bark	3	51.84	6.14	40.97	0.34	0.02	99.31
Needles	4	50.22	6.22	38.77	0.92	0.09	96.22
Bark + needles	5	50.35	6.18	40.21	0.67	0.06	97.47
Residues (rep 1)	8	49.82	6.56	41.34	0.58	0.05	98.35
Residues:bark:needles 1:1:1	10	50.58	6.31	40.43	0.59	0.05	97.96
Residues:bark:needles 1:2:2	11	50.86	6.24	40.24	0.58	0.06	97.98
Air classified (10 Hz)	12	50.16	6.46	42.06	0.37	0.03	99.08
Air classified (28 Hz)	13	48.93	6.42	43.77	0.26	0.02	99.40
Whole tree (13 yr)	15	49.32	6.44	43.48	0.30	0.02	99.56
Stem wood (13 yr)	16	49.40	6.41	43.68	0.21	0.01	99.71
Maximum difference		2.95	0.42	5.35	0.74	0.08	

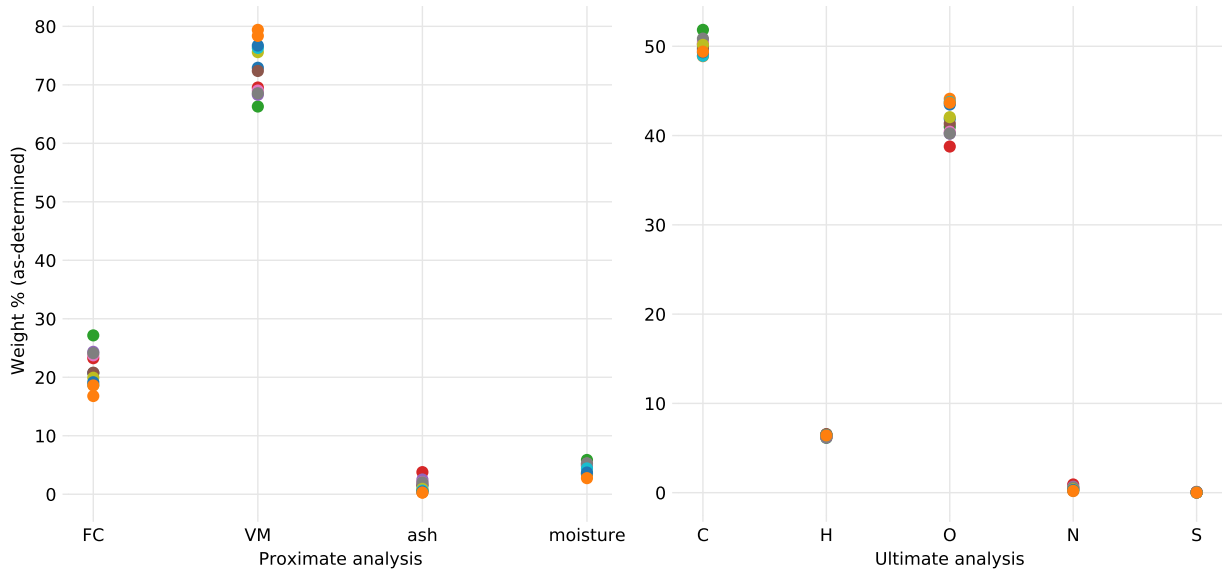

Figure 3: Comparison of proximate (left) and ultimate (right) analysis measurements for each feedstock. Values represent wt. % as-determined basis.

The proximate analysis data was converted to different bases using ASTM methods [1]. Equations 1–4 convert the as-determined (ad) basis to as-received (ar), dry (d), and dry ash-free (daf) bases where X is the wt. % of the corresponding basis value, M is the moisture content, and ADL is the air-dry loss assumed to be 22 wt. %. As an example, to obtain the as-received value of the fixed carbon use $FC_{ar} = FC_{ad} \times \frac{100-M_{ar}}{100-M_{ad}}$.

$$M_{ar} = \left(M_{ad} \times \frac{100 - ADL}{100}\right) + ADL \tag{1}$$

$$X_{ar} = X_{ad} \times \frac{100 - M_{ar}}{100 - M_{ad}} \tag{2}$$

$$X_{d} = X_{ad} \times \frac{100}{100 - M_{ad}} \tag{3}$$

$$X_{daf} = X_{ad} \times \frac{100}{100 - M_{ad} - ash_{ad}} \tag{4}$$

Similarly, the ultimate analysis data was also converted to different bases using the ASTM methods [1]. Equations 1–4 convert the carbon, nitrogen, and sulfur fractions to different bases while Equations 5–8 are for the hydrogen and oxygen fractions. Equation 9 calculates the CHO basis from the dry ash-free basis.

$$H_{ar} = (H_{ad} - 0.1119\,M_{ad}) \times \frac{100 - M_{ar}}{100 - M_{ad}} \tag{5}$$

$$O_{ar} = (O_{ad} - 0.8881\,M_{ad}) \times \frac{100 - M_{ar}}{100 - M_{ad}} \tag{6}$$

$$H_{d} = (H_{ad} - 0.1119\,M_{ad}) \times \frac{100}{100 - M_{ad}} \tag{7}$$

$$O_{d} = (O_{ad} - 0.8881\,M_{ad}) \times \frac{100}{100 - M_{ad}} \tag{8}$$

$$X_{cho} = X_{daf} \times \frac{100}{100 - N_{daf} - S_{daf}} \tag{9}$$

Table 5 presents the proximate and ultimate analysis data on an as-determined (ad), as-received (ar), dry (d), dry ash-free (daf), and CHO basis. The reported H and O for the ultimate analysis data does not include the H and O in the moisture; therefore, the total value for the as-determined basis excludes the moisture percentage for the ultimate analysis.

Table 5: Proximate and ultimate analysis basis values for each feedstock given as wt. %. Reported H and O values for ultimate analysis ad-basis excludes H and O in moisture.

Residues	ad	ar	d	daf	cho
FC	20.72	17.33	21.79	22.13	–
VM	72.92	60.99	76.69	77.88	–
ash	1.45	1.21	1.53	–	–
moisture	4.92	20.58	–	–	–
total	100.01	100.01	100.01	100.01	–
C	49.63	38.71	52.20	53.01	53.31
H	6.52	4.66	6.28	6.38	6.41
O	41.87	29.25	39.44	40.05	40.28
N	0.49	0.38	0.52	0.52	–
S	0.04	0.03	0.04	0.04	–
ash	1.45	1.13	1.53	–	–
moisture	(4.92)	25.84	–	–	–
total	100	100	100	100	100
Stem wood	ad	ar	d	daf	cho
FC	16.79	13.10	17.41	17.46	–
VM	79.40	61.93	82.32	82.56	–
ash	0.28	0.22	0.29	–	–
moisture	3.55	24.77	–	–	–
total	100.02	100.02	100.02	100.02	–
C	48.89	38.13	50.69	50.84	50.94
H	6.53	4.78	6.36	6.38	6.39
O	44.12	31.95	42.48	42.60	42.68
N	0.18	0.14	0.19	0.19	–
S	0.01	0.01	0.01	0.01	–
ash	0.28	0.22	0.29	–	–
moisture	(3.55)	24.77	–	–	–
total	100.01	100.01	100.01	100.01	100.01
Bark	ad	ar	d	daf	cho
FC	27.16	21.18	28.85	29.07	–
VM	66.29	51.71	70.42	70.94	–
ash	0.70	0.55	0.74	–	–
moisture	5.86	26.57	–	–	–
total	100.01	100.01	100.01	100.01	–

C	51.84	40.44	55.07	55.48	55.69
H	6.14	4.28	5.83	5.87	5.89
O	40.97	27.90	37.99	38.28	38.42
N	0.34	0.27	0.36	0.36	–
S	0.02	0.02	0.02	0.02	–
ash	0.70	0.55	0.74	–	–
moisture	(5.86)	26.57	–	–	–
total	100.01	100.01	100.01	100.01	100.01

Needles	ad	ar	d	daf	cho
FC	23.26	18.14	24.08	25.06	–
VM	69.54	54.24	72.00	74.94	–
ash	3.78	2.95	3.91	–	–
moisture	3.42	24.67	–	–	–
total	100	100	100	100	–
C	50.22	39.17	52.00	54.12	54.71
H	6.22	4.55	6.04	6.29	6.36
O	38.77	27.87	37.00	38.51	38.93
N	0.92	0.72	0.95	0.99	–
S	0.09	0.07	0.09	0.10	–
ash	3.78	2.95	3.91	–	–
moisture	(3.42)	24.67	–	–	–
total	100	100	100	100	100

Bark + needles	ad	ar	d	daf	cho
FC	24.35	18.99	25.59	26.29	–
VM	68.30	53.27	71.78	73.73	–
ash	2.52	1.97	2.65	–	–
moisture	4.85	25.78	–	–	–
total	100.02	100.02	100.02	10.02	–
C	50.35	39.27	52.92	54.36	54.79
H	6.18	4.40	5.92	6.09	6.13
O	40.21	28.00	37.73	38.76	39.07
N	0.67	0.52	0.70	0.72	–
S	0.06	0.05	0.06	0.06	–
ash	2.52	1.97	2.65	–	–
moisture	(4.85)	25.78	–	–	–
total	99.99	99.99	99.99	99.99	99.99

Residues (rep 1)	ad	ar	d	daf	cho

FC	20.78	16.21	21.92	22.31	–
VM	72.37	56.45	76.34	77.69	–
ash	1.65	1.29	1.74	–	–
moisture	5.20	26.06	–	–	–
total	100	100	100	100	–
C	49.82	38.86	52.55	53.48	53.85
H	6.56	4.66	6.31	6.42	6.46
O	41.34	28.64	38.74	39.42	39.69
N	0.58	0.45	0.61	0.62	–
S	0.05	0.04	0.05	0.05	–
ash	1.65	1.29	1.74	–	–
moisture	(5.20)	26.06	–	–	–
total	100	100	100	100	100
Residues:bark:needles 1:1:1	ad	ar	d	daf	cho
FC	23.75	18.52	25.05	25.60	–
VM	69.02	53.84	72.80	74.41	–
ash	2.05	1.60	2.16	–	–
moisture	5.19	26.05	–	–	–
total	100.01	100.01	100.01	100.01	–
C	50.58	39.45	53.35	54.53	54.91
H	6.31	4.47	6.04	6.18	6.22
O	40.43	27.94	37.78	38.62	38.88
N	0.59	0.46	0.62	0.64	–
S	0.05	0.04	0.05	0.05	–
ash	2.05	1.60	2.16	–	–
moisture	(5.19)	26.05	–	–	–
total	100.01	100.01	100.01	100.01	100.01
Residues:bark:needles 1:2:2	ad	ar	d	daf	cho
FC	24.12	18.81	25.47	26.02	–
VM	68.57	53.48	72.40	73.98	–
ash	2.02	1.58	2.13	–	–
moisture	5.29	26.13	–	–	–
total	100	100	100	100	–
C	50.86	39.67	53.70	54.87	55.25
H	6.24	4.41	5.96	6.09	6.14
O	40.24	27.72	37.53	38.34	38.61

N	0.58	0.45	0.61	0.63	–
S	0.06	0.05	0.06	0.06	–
ash	2.02	1.58	2.13	–	–
moisture	(5.29)	26.13	–	–	–
total	100	100	100	100	100
Air classified 10 Hz	ad	ar	d	daf	cho
FC	19.92	15.54	20.66	20.86	–
VM	75.59	58.96	78.39	79.14	–
ash	0.92	0.72	0.95	–	–
moisture	3.57	24.78	–	–	–
total	100	100	100	100	–
C	50.16	39.12	52.02	52.52	52.74
H	6.46	4.73	6.28	6.35	6.37
O	42.06	30.33	40.33	40.72	40.89
N	0.37	0.29	0.38	0.39	–
S	0.03	0.02	0.03	0.03	–
ash	0.92	0.72	0.95	–	–
moisture	(3.57)	24.78	–	–	–
total	100	100	100	100	100
Air classified 28 Hz	ad	ar	d	daf	cho
FC	18.68	14.57	19.54	19.67	–
VM	76.31	59.52	79.83	80.34	–
ash	0.61	0.48	0.64	–	–
moisture	4.41	25.44	–	–	–
total	100.01	100.01	100.01	100.01	–
C	48.93	38.17	51.19	51.52	51.67
H	6.42	4.62	6.20	6.24	6.26
O	43.77	31.09	41.69	41.96	42.08
N	0.26	0.20	0.27	0.27	–
S	0.02	0.02	0.02	0.02	–
ash	0.61	0.48	0.64	–	–
moisture	(4.41)	25.44	–	–	–
total	100.01	100.01	100.01	100.01	100.01
Whole tree 13 yr	ad	ar	d	daf	cho
FC	19.15	14.94	19.89	19.98	–
VM	76.72	59.84	79.68	80.04	–

ash	0.44	0.34	0.46	–	–
moisture	3.71	24.89	–	–	–
total	100.02	100.02	100.02	100.02	–
C	49.32	38.47	51.22	51.46	51.63
H	6.44	4.70	6.26	6.29	6.31
O	43.48	31.34	41.73	41.93	42.07
N	0.30	0.23	0.31	0.31	–
S	0.02	0.02	0.02	0.02	–
ash	0.44	0.34	0.46	–	–
moisture	(3.71)	24.89	–	–	–
total	100	100	100	100	100
Stem wood 13 yr	ad	ar	d	daf	cho
FC	18.60	14.51	19.13	19.19	–
VM	78.37	61.13	80.59	80.84	–
ash	0.30	0.23	0.31	–	–
moisture	2.75	24.14	–	–	–
total	100.02	100.02	100.02	100.02	–
C	49.40	38.53	50.80	50.95	51.07
H	6.41	4.76	6.27	6.29	6.31
O	43.68	32.17	42.40	42.54	42.63
N	0.21	0.16	0.22	0.22	–
S	0.01	0.01	0.01	0.01	–
ash	0.30	0.23	0.31	–	–
moisture	(2.75)	24.14	–	–	–
total	100.01	100.01	100.01	100.01	100.01

2.3 Feedstock chemical analysis

Chemical analysis data for each feedstock was supplied by INL on a wt. % dry basis (d). The dry basis values P_d are converted to a dry ash-free basis P_{daf} using Equation 10 where $P_{s.inorg.}$ is the structural inorganics and $P_{ns.inorg.}$ is the non-structural inorganics. A summary of the chemical analysis data and converted values are presented in Table 6 while a comparison of the as-determined values are shown in Figure 4. The largest variations in the measured chemical fractions occur for the lignin and glucan with a maximum difference of 15 wt. % and 17.5 wt. % respectively.

$$P_{daf} = P_d \times \frac{100}{\sum P_d - P_{s.inorg.} - P_{ns.inorg.}} \tag{10}$$

Table 6: Chemical analysis values shown as weight percent (wt. %) for dry (d) and dry ash-free (daf) bases.

Residues, Cycle 1	d	daf
structural inorganics	0.94	–
non-structural inorganics	0.37	–
water extractives	4.91	5.05
ethanol extractives	0.62	0.64
acetone extractives	6.6	6.79
lignin	35.52	36.53
glucan	28.18	28.98
xylan	7.33	7.54
galactan	3.56	3.66
arabinan	1.93	1.98
mannan	7.64	7.86
acetyl	0.95	0.98
total	98.55	100

Stem wood, Cycle 2	d	daf
structural inorganics	0.32	–
non-structural inorganics	0	–
water extractives	2.76	2.72
ethanol extractives	0.31	0.31
acetone extractives	2.57	2.54
lignin	30.7	30.29
glucan	39.84	39.31
xylan	6.3	6.22
galactan	2.59	2.56
arabinan	0	0
mannan	14.94	14.74
acetyl	1.35	1.33
total	101.68	100

Bark, Cycle 3	d	daf
structural inorganics	0.5	–
non-structural inorganics	0.08	–
water extractives	2.9	2.90
ethanol extractives	0.46	0.46
acetone extractives	3.33	3.33
lignin	34.34	34.29
glucan	33.83	33.78
xylan	7.74	7.73
galactan	3.68	3.67
arabinan	3.5	3.50

mannan	9.15	9.14
acetyl	1.21	1.21
total	100.72	100

Needles, Cycle 4	d	daf
structural inorganics	3.23	–
non-structural inorganics	0.56	–
water extractives	5.95	6.29
ethanol extractives	1.35	1.43
acetone extractives	7.35	7.77
lignin	41.03	43.35
glucan	22.33	23.59
xylan	4.12	4.35
galactan	2.57	2.72
arabinan	1.52	1.61
mannan	7.44	7.86
acetyl	0.98	1.04
total	98.43	100

Bark + needles, Cycle 5	d	daf
structural inorganics	1.76	–
non-structural inorganics	0.66	–
water extractives	4.01	4.21
ethanol extractives	0.98	1.03
acetone extractives	5.53	5.81
lignin	45.88	48.21
glucan	22.75	23.91
xylan	4.17	4.38
galactan	3.28	3.45
arabinan	2.4	2.52
mannan	5.35	5.62
acetyl	0.81	0.85
total	97.58	100

Residues (rep 1), Cycle 8	d	daf
structural inorganics	1.24	–
non-structural inorganics	0.19	–
water extractives	6.18	6.40
ethanol extractives	0.68	0.70
acetone extractives	7.88	8.16
lignin	35.22	36.49
glucan	26.48	27.44
xylan	6.52	6.76

galactan	3.44	3.56
arabinan	2.84	2.94
mannan	6.33	6.56
acetyl	0.94	0.97
total	97.94	100

Residues:bark:needles 1:1:1, Cycle 10	d	daf
structural inorganics	1.66	–
non-structural inorganics	0.02	–
water extractives	5.76	5.93
ethanol extractives	1.02	1.05
acetone extractives	6.87	7.07
lignin	42.06	43.28
glucan	23.37	24.05
xylan	5.07	5.22
galactan	2.95	3.04
arabinan	1.62	1.67
mannan	7.55	7.77
acetyl	0.9	0.93
total	98.85	100

Residues:bark:needles 1:2:2, Cycle 11	d	daf
structural inorganics	1.91	–
non-structural inorganics	0.21	–
water extractives	5.53	5.79
ethanol extractives	1.04	1.09
acetone extractives	6.51	6.81
lignin	42.9	44.89
glucan	22.92	23.98
xylan	4.64	4.86
galactan	3.03	3.17
arabinan	2.23	2.33
mannan	5.91	6.18
acetyl	0.85	0.89
total	97.68	100

Air classified (10 Hz), Cycle 12	d	daf
structural inorganics	0.55	–
non-structural inorganics	0.31	–
water extractives	3.26	3.31
ethanol extractives	0.44	0.45
acetone extractives	4.02	4.08
lignin	35.11	35.60

glucan	31.99	32.44
xylan	7.63	7.74
galactan	3.63	3.68
arabinan	1.34	1.36
mannan	10.01	10.15
acetyl	1.18	1.20
total	99.47	100

Air classified (28 Hz), Cycle 13	d	daf
structural inorganics	0.38	–
non-structural inorganics	0.22	–
water extractives	1.76	1.76
ethanol extractives	0.31	0.31
acetone extractives	2.4	2.40
lignin	35.23	35.23
glucan	34.37	34.37
xylan	8.39	8.39
galactan	3.9	3.90
arabinan	0	0
mannan	12.41	12.41
acetyl	1.24	1.24
total	100.61	100

Whole tree (13 yr), Cycle 15	d	daf
structural inorganics	0.5	–
non-structural inorganics	0.08	–
water extractives	2.9	2.93
ethanol extractives	0.46	0.46
acetone extractives	3.33	3.36
lignin	33.34	33.63
glucan	33.83	34.12
xylan	7.74	7.81
galactan	3.68	3.71
arabinan	3.5	3.53
mannan	9.15	9.23
acetyl	1.21	1.22
total	99.72	100

Stem wood (13 yr), Cycle 16	d	daf
structural inorganics	0.32	–
non-structural inorganics	0	–
water extractives	1.56	1.53
ethanol extractives	0.34	0.33

acetone extractives	1.76	1.73
lignin	33.4	32.80
glucan	38.15	37.46
xylan	7.97	7.83
galactan	3.63	3.56
arabinan	3.53	3.47
mannan	10.08	9.90
acetyl	1.41	1.38
total	102.15	100

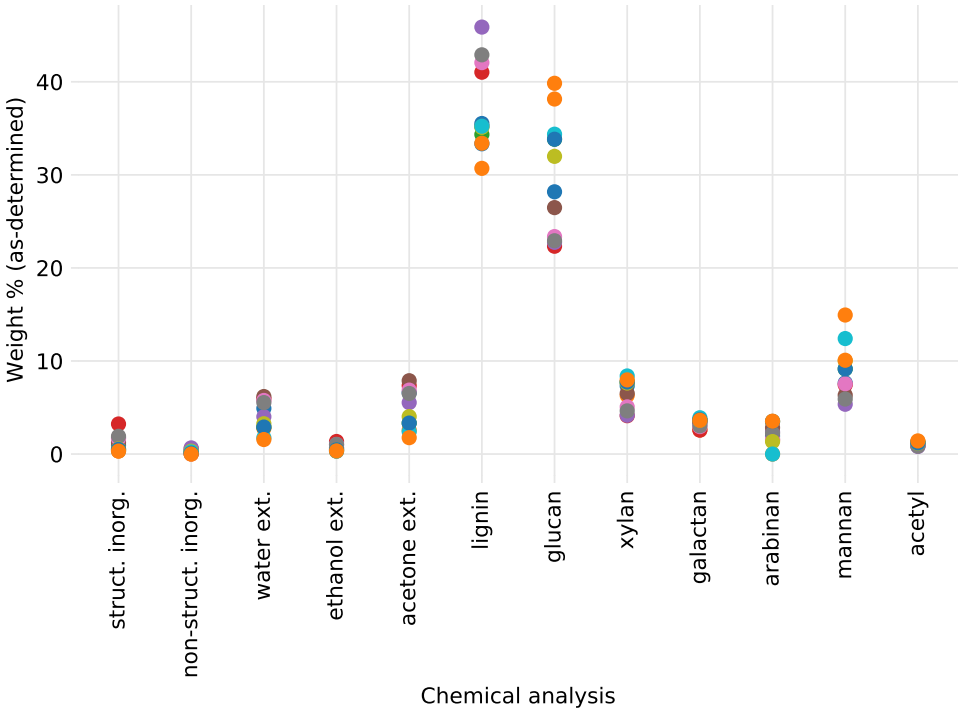

Figure 4: Comparison of chemical analysis measurements for each feedstock.

2.4 Bed particle characteristics

Characteristics of the sand particles that represent the fluidized bed material were obtained by NETL and are summarized in Table 7. A microscope image of the sand particles is shown in Figure 5. The particle density was determined from a helium pycnometer while size distribution and sphericity was obtained from QICPIC image analysis [6]. At the time of writing this report, bed particle characteristics were not utilized in the reactor models discussed in subsequent sections.

Table 7: Bed material (sand) characteristics.

Parameter	Symbol	Value	Units
Particle envelope density	ρ	2.7051	g/cm^3
Standard deviation of density	–	0.0004	g/cm^3
Sauter mean diameter	SMD	509	μm
Average particle sphericity	ϕ	0.874	–

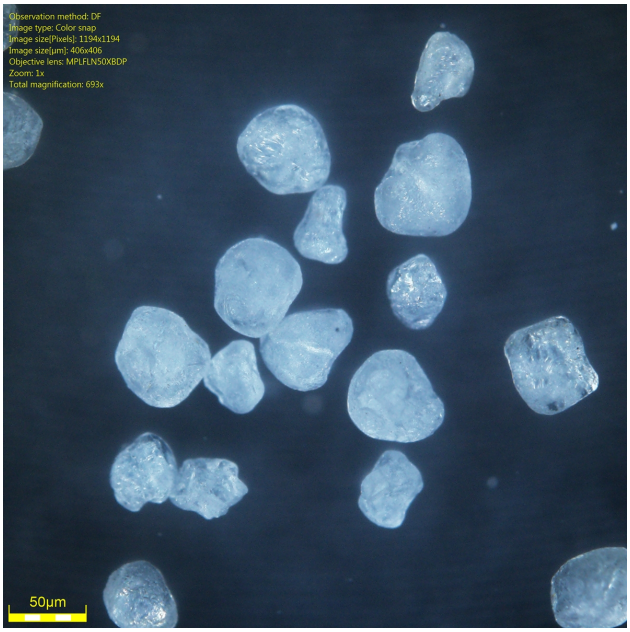

Figure 5: Microscope image of sand particles used for the bed material.

2.5 Product yields

Product yields measured from the fast pyrolysis of each feedstock in the fluidized bed reactor are given in Table 8. A comparison of the product yields from each feedstock is shown in Figure 6. The oil and char yields are the most variable between the different feedstocks while condensables and water vapor differ by a few percent.

Table 8: Measured reactor yields from each feedstock experiment. Values expressed as percent wet basis (w).

Feedstock	Oil	Condensables	Light gas	Water vapor	Char	Total
Residues	63.5	1.6	14.7	0.4	15.2	95.4
Stem wood	72.3	2.8	14.1	1.2	10.9	101.3
Bark	58.3	1.3	11.4	0.8	31.9	103.7
Needles	55.4	2.7	14.5	0.6	25.6	98.8
Bark + needles	55.5	1.3	15.1	1.2	16.5	89.6
Residues (rep 1)	62.6	2.5	15.9	2.5	17.3	100.8
Residues:bark:needles 1:1:1	58.3	3.1	14.3	0.7	24.6	101.0
Residues:bark:needles 1:2:2	57.1	0.6	15.0	2.0	25.0	99.7
Air classified (10 Hz)	57.6	3.0	16.2	3.2	16.3	96.3
Air classified (28 Hz)	65.0	2.5	17.9	1.6	13.9	100.9
Whole tree (13 yr)	63.1	1.8	17.7	2.1	13.9	98.6
Stem wood (13 yr)	67.8	1.9	15.2	3.2	12.2	100.3

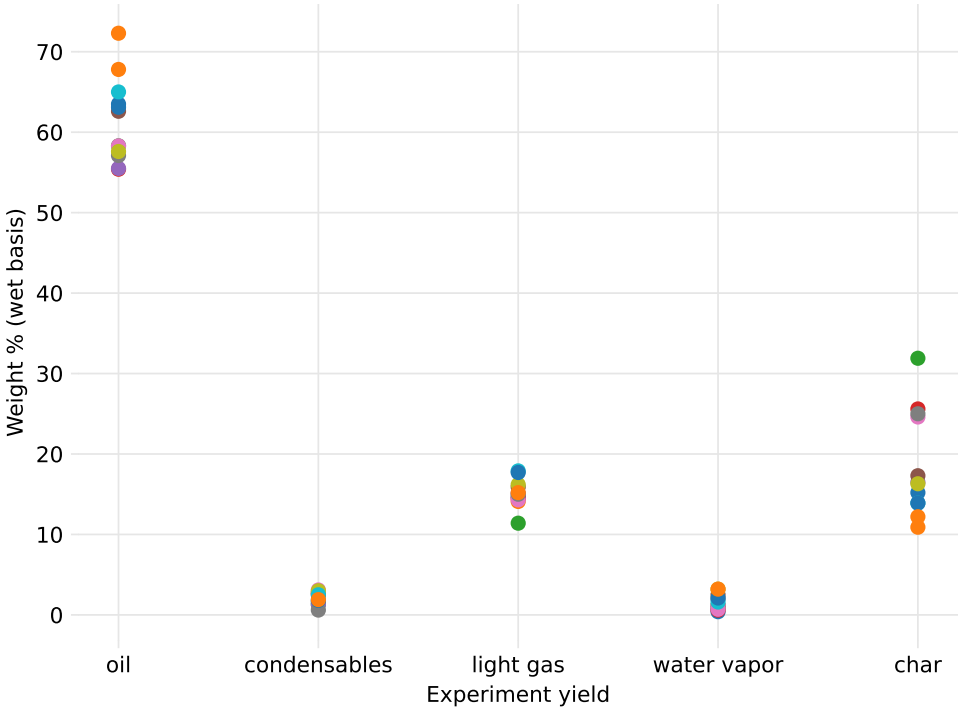

Figure 6: Comparison of the measured product yields for each feedstock. Values shown as percent wet basis.

3 Model development

This section details the biomass pyrolysis kinetics scheme, biomass composition characterization method, and the reduced-order reactor models.

3.1 Biomass pyrolysis kinetics

The kinetic reaction mechanisms presented in the Debiagi et al. 2018 paper [2] were used to model biomass pyrolysis in the fluidized bed reactor. Table 9 summarizes the reactions along with the associated prefactors and activation energies. A description of the chemical species in the Debiagi et al. kinetic scheme is provided in Table 10. Species are grouped into solid, metaplastic, gas, and liquid phases. Solid and metaplastic species are combined and compared to the reactor's char yield. All liquid species are combined and compared to the reactor's total liquid yield.

Table 9: Kinetic reactions for biomass pyrolysis where A is the prefactor, E is the activation energy, and T is temperature. Source [2].

Item	Reaction	A (1/s)	E (cal/mol)
1	CELL → CELLA	1.5×10^{14}	47,000
2	CELLA → 0.40 CH2OHCHO + 0.03 CHOCHO + 0.17 CH3CHO + 0.25 C6H6O3 + 0.35 C2H5CHO + 0.20 CH3OH + 0.15 CH2O + 0.49 CO + 0.05 G{CO} + 0.43 CO2 + 0.13 H2 + 0.93 H2O + 0.05 G{COH2} loose + 0.02 HCOOH + 0.05 CH2OHCH2CHO + 0.05 CH4 + 0.1 G{H2} + 0.66 CHAR	2.5×10^{6}	19,100
3	CELLA → C6H10O5	3.3 × T	10,000
4	CELL → 4.45 H2O + 5.45 CHAR + 0.12 G{COH2} stiff + 0.18 G{COH2} loose + 0.25 G{CO} + 0.125 G{H2} + 0.125 H2	9.0×10^{7}	31,000
5	GMSW → 0.70 HCE1 + 0.30 HCE2	1.0×10^{10}	31,000
6	XYHW → 0.35 HCE1 + 0.65 HCE2	1.25×10^{11}	31,400
7	XYGR → 0.12 HCE1 + 0.88 HCE2	1.25×10^{11}	30,000
8	HCE1 → 0.25 C5H8O4 + 0.25 C6H10O5 + 0.16 FURFURAL + 0.13 C6H6O3 + 0.09 CO2 + 0.1 CH4 + 0.54 H2O + 0.06 CH2OHCH2CHO + 0.1 CHOCHO + 0.02 H2 + 0.1 CHAR	16.0 × T	12,900
9	HCE1 → 0.4 H2O + 0.39 CO2 + 0.05 HCOOH + 0.49 CO + 0.01 G{CO} + 0.51 G{CO2} + 0.05 G{H2} + 0.4 CH2O + 0.43 G{COH2} loose + 0.3 CH4 + 0.325 G{CH4} + 0.1 C2H4 + 0.075 G{C2H4} + 0.975 CHAR + 0.37 G{COH2} stiff + 0.1 H2 + 0.2 G{C2H6}	$3.0 \times 10^{-3} \times$ T	3,600
10	HCE2 → 0.3 CO + 0.5125 CO2 + 0.1895 CH4 + 0.5505 H2 + 0.056 H2O + 0.049 C2H5OH + 0.035 CH2OHCHO + 0.105 CH3CO2H + 0.0175 HCOOH + 0.145 FURFURAL + 0.05 G{CH4} + 0.105 G{CH3OH} + 0.1 G{C2H4} + 0.45 G{CO2} + 0.18 G{COH2} loose + 0.7125 CHAR + 0.21 G{H2} + 0.78 G{COH2} stiff + 0.2 G{C2H6}	7.0×10^{9}	30,500
11	LIGH → LIGOH + 0.5 C2H5CHO + 0.4 C2H4 + 0.2 CH2OHCHO + 0.1 CO + 0.1 C2H6	6.7×10^{12}	37,500
12	LIGO → LIGOH + CO2	3.3×10^{8}	25,500
13	LIGC → 0.35 LIGCC + 0.1 VANILLIN + 0.1 C6H5OCH3 + 0.27 C2H4 + H2O + 0.17 G{COH2} loose + 0.4 G{COH2} stiff + 0.22 CH2O + 0.21 CO + 0.1 CO2 + 0.36 G{CH4} + 5.85 CHAR + 0.2 G{C2H6} + 0.1 G{H2}	1.0×10^{11}	37,200

14	LIGCC → 0.25 VANILLIN + 0.15 CRESOL + 0.15 C6H5OCH3 + 0.35 CH2OHCHO + 0.7 H2O + 0.45 CH4 + 0.3 C2H4 + 0.7 H2 + 1.15 CO + 0.4 G{CO} + 6.80 CHAR + 0.4 C2H6	1.0×10^4	24,800
15	LIGOH → 0.9 LIG + H2O + 0.1 CH4 + 0.6 CH3OH + 0.3 G{CH3OH} + 0.05 CO2 + 0.65 CO + 0.6 G{CO} + 0.05 HCOOH + 0.45 G{COH2} loose + 0.4 G{COH2} stiff + 0.25 G{CH4} + 0.1 G{C2H4} + 0.15 G{C2H6} + 4.25 CHAR + 0.025 C24H28O4 + 0.1 C2H3CHO	1.5×10^8	30,000
16	LIG → VANILLIN + 0.1 C6H5OCH3 + 0.5 C2H4 + 0.6 CO + 0.3 CH3CHO + 0.1 CHAR	$4.0 \times T$	12,000
17	LIG → 0.6 H2O + 0.3 CO + 0.1 CO2 + 0.2 CH4 + 0.4 CH2O + 0.2 G{CO} + 0.4 G{CH4} + 0.5 G{C2H4} + 0.4 G{CH3OH} + 1.25 G{COH2} loose + 0.65 G{COH2} stiff + 6.1 CHAR + 0.1 G{H2}	$8.3 \times 10^{-2} \times T$	8,000
18	LIG → 0.6 H2O + 2.6 CO + 0.6 CH4 + 0.4 CH2O + 0.75 C2H4 + 0.4 CH3OH + 4.5 CHAR + 0.5 C2H6	1.5×10^9	31,500
19	TGL → C2H3CHO + 2.5 MLINO + 0.5 U2ME12	7.0×10^{12}	45,700
20	TANN → 0.85 C6H5OH + 0.15 G{C6H5OH} + G{CO} + H2O + ITANN	2.0×10^1	10,000
21	ITANN → 5 CHAR + 2 CO + H2O + 0.55 G{COH2} loose + 0.45 G{COH2} stiff	1.0×10^3	25,000
22	G{CO2} → CO2	1.0×10^6	24,500
23	G{CO} → CO	5.0×10^{12}	52,500
24	G{CH3OH} → CH3OH	2.0×10^{12}	50,000
25	G{COH2}loose → 0.2 CO + 0.2 H2 + 0.8 H2O + 0.8 CHAR	6.0×10^{10}	50,000
26	G{C2H6} → C2H6	1.0×10^{11}	52,000
27	G{CH4} → CH4	1.0×10^{11}	53,000
28	G{C2H4} → C2H4	1.0×10^{11}	54,000
29	G{C6H5OH} → C6H5OH	1.5×10^{12}	55,000
30	G{COH2}stiff → 0.8 CO + 0.8 H2 + 0.2 H2O + 0.2 CHAR	1.0×10^9	59,000
31	G{H2} → H2	1.0×10^8	70,000
32	ACQUA → H2O	$1.0 \times T$	8,000

Table 10: Description of the chemical species in the Debiagi kinetics scheme for biomass pyrolysis. Source [2].

Item	Name	Formula	Phase	Description
1	CELL	$C_6H_{10}O_5$	solid	cellulose
2	CELLA	$C_6H_{10}O_5$	solid	active cellulose
3	GMSW	$C_5H_8O_4$	solid	hemicellulose softwood
4	XYHW	$C_5H_8O_4$	solid	hemicellulose hardwood
5	XYGR	$C_5H_8O_4$	solid	hemicellulose grass
6	HCE1	$C_5H_8O_4$	solid	intermediate hemicellulose
7	HCE2	$C_5H_8O_4$	solid	intermediate hemicellulose
8	ITANN	$C_8H_4O_4$	solid	intermediate phenolics
9	LIG	$C_{11}H_{12}O_4$	solid	intermediate lignin
10	LIGC	$C_{15}H_{14}O_4$	solid	carbon rich lignin
11	LIGCC	$C_{15}H_{14}O_4$	solid	intermediate lignin
12	LIGH	$C_{22}H_{28}O_9$	solid	hydrogen rich lignin
13	LIGO	$C_{20}H_{22}O_{10}$	solid	oxygen rich lignin
14	LIGOH	$C_{19}H_{22}O_8$	solid	intermediate lignin

15	TANN	$C_{15}H_{12}O_7$	solid	tannins
16	TGL	$C_{57}H_{100}O_7$	solid	triglycerides
17	CHAR	C	solid	char as pure carbon
18	ACQUA	H_2O	solid	biomass moisture content
19	G{COH2} loose	CH_2O	metaplastic	loose formaldehyde
20	G{CO2}	CO_2	metaplastic	trapped carbon dioxide
21	G{CO}	CO	metaplastic	trapped carbon monoxide
22	G{CH3OH}	CH_4O	metaplastic	trapped methanol
23	G{CH4}	CH_4	metaplastic	trapped methane
24	G{C2H4}	C_2H_4	metaplastic	trapped ethylene
25	G{C6H5OH}	C_6H_6O	metaplastic	trapped phenol
26	G{COH2} stiff	CH_2O	metaplastic	stiff formaldehyde
27	G{H2}	H_2	metaplastic	trapped hydrogen
28	G{C2H6}	C_2H_6	metaplastic	trapped ethane
29	C2H4	C_2H_4	gas	ethylene
30	C2H6	C_2H_6	gas	ethane
31	CH2O	CH_2O	gas	formaldehyde
32	CH4	CH_4	gas	methane
33	CO	CO	gas	carbon monoxide
34	CO2	CO_2	gas	carbon dioxide
35	H2	H_2	gas	hydrogen
36	C2H3CHO	C_3H_4O	liquid	acrolein
37	C2H5CHO	C_3H_6O	liquid	propionaldehyde
38	C2H5OH	C_2H_6O	liquid	ethanol
39	C5H8O4	$C_5H_8O_4$	liquid	xylofuranose
40	C6H10O5	$C_6H_{10}O_5$	liquid	levoglucosan
41	C6H5OCH3	C_7H_8O	liquid	anisole
42	C6H5OH	C_6H_6O	liquid	phenol
43	C6H6O3	$C_6H_6O_3$	liquid	hydroxymethylfurfural
44	C24H28O4	$C_{24}H_{28}O_4$	liquid	heavy molecular weight lignin
45	CH2OHCH2CHO	$C_3H_6O_2$	liquid	propionic acid
46	CH2OHCHO	$C_2H_4O_2$	liquid	acetic acid
47	CH3CHO	C_2H_4O	liquid	acetaldehyde
48	CH3CO2H	$C_2H_4O_2$	liquid	acetic acid
49	CH3OH	CH_4O	liquid	methanol
50	CHOCHO	$C_2H_2O_2$	liquid	glyoxal
51	CRESOL	C_7H_8O	liquid	cresol
52	FURFURAL	$C_5H_4O_2$	liquid	2-furaldehyde
53	H2O	H_2O	liquid	water from reactions
54	HCOOH	CH_2O_2	liquid	formic acid
55	MLINO	$C_{19}H_{34}O_2$	liquid	methyl linoleate
56	U2ME12	$C_{13}H_{22}O_2$	liquid	linalyl propionate
57	VANILLIN	$C_8H_8O_3$	liquid	vanillin

3.2 Biomass composition

The Debiagi kinetics rely on an initial biomass composition defined as cellulose (CELL), hemicellulose (HCELL), carbon-rich lignin (LIGC), hydrogen-rich lignin (LIGH), oxygen-rich lignin (LIGO), tannins (TANN), and triglycerides (TGL). The hemicellulose reaction mechanisms consider different types of biomass such as softwood (GMSW), hardwood

(XYHW), and grass (XYGR) feedstocks. Figure 7 illustrates the conversion of the biomass components to pyrolysis products of liquids, solids, metaplastics, and gases as discussed in the Debiagi et al. kinetics scheme.

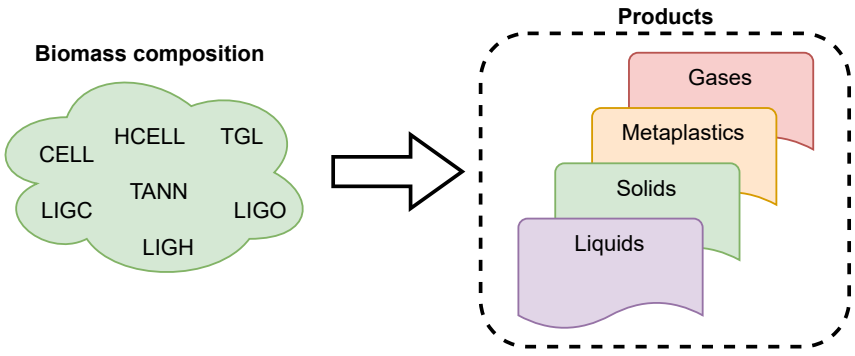

Figure 7: Seven biomass components convert to pyrolysis products according to the Debiagi et al. biomass pyrolysis kinetics scheme.

According to the Debiagi et al. 2015 paper [3], the chemical components of the biomass are defined as shown in Table 11. The Debiagi paper does not provide information on how to experimentally determine these components. However, the paper provides a characterization method which estimates the biomass composition based on elemental (ultimate) analysis data. The characterization method uses the carbon (C) and hydrogen (H) content of the biomass to predict the biochemical composition in terms of cellulose, hemicellulose, lignin, tannins, and triglycerides. Splitting parameters α, β, γ, δ, and ϵ are used to improve the validity of the characterization procedure by accounting for extractives in the biomass.

Table 11: Chemical components representing biomass composition needed for the Debiagi et al. pyrolysis kinetics.

Biomass composition	Symbol	Description
cellulose	CELL	glucan
hemicellulose	GMSW XYHW XYGR	mixture of sugars such as hexoses and pentoses; mainly xylose, mannose, galactose, and arabinose
lignin	LIG	aromatic alcohols such as coniferyl, sinapyl, p-coumaryl alcohol
lignin-c	LIG-C	carbon-rich lignin
lignin-h	LIG-H	hydrogen-rich lignin
lignin-o	LIG-O	oxygen-rich lignin
tannins	TANN	hydrophilic extractives, phenolics, ethanol and water, represented by a gallocatechin polymer
triglycerides	TGL	hydrophobic extractives, hexane and ether, linoleic acid

As discussed previously, the largest differences in the chemical analysis feedstock data are for the lignin, glucan, and mannan fractions. These fractions represent the cellulose (glucan), hemicellulose (xylan, galactan, arabinan, mannan, acetyl), and total lignin components of the biomass composition. Unfortunately, the chemical analysis data does not directly relate to all the biomass components needed for the pyrolysis kinetics.

Using the C and H values from the ultimate analysis data and default values for the splitting parameters, the biomass composition is estimated using the characterization method from Debiagi et al. The estimated cellulose, hemicellulose, and total lignin (LIGC + LIGH + LIGO) values are compared to the chemical analysis data using a minimization function

$$\sum (a-b)^2 \tag{11}$$

where a is the cellulose, hemicellulose, and total lignin estimated from the characterization method and b is the cellulose, hemicellulose, and lignin from the chemical analysis data. The L-BFGS-B algorithm is applied to the minimization function to generate the optimum splitting parameter values such that the cellulose, hemicellulose, and total lignin are similar to the values obtained from the chemical analysis data.

Figure 8 demonstrates the biomass composition procedure while Table 12 presents the biomass compositions for each FCIC feedstock that is suitable to use with the Debiagi et al. kinetics scheme. As seen in the table, the optimization procedure is able to determine the appropriate splitting parameters when comparing the biomass composition to chemical analysis data. The biomass composition for the bark feedstock is the only composition that does not compare within 1% of the chemical analysis values.

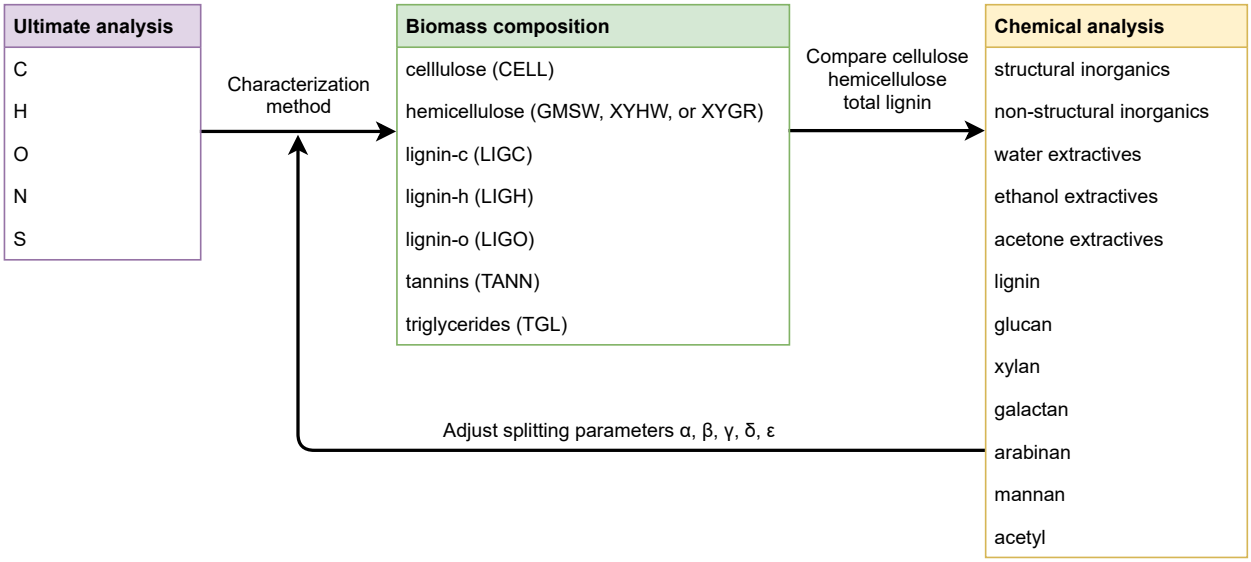

Figure 8: Biomass composition determined from ultimate analysis data and compared with measured chemical analysis data for cellulose, hemicellulose, and total lignin.

Table 12: Estimated biomass composition for each feedstock on a dry ash-free basis (daf). Left daf column based on chemical analysis data. Right daf column estimated from the characterization procedure using the optimized splitting parameter values.

Residues, Cycle 1	daf	daf
cellulose	28.98	28.98
hemicellulose	22.02	22.02
lignin-c	–	0.58
lignin-h	–	8.79
lignin-o	–	27.16
tannins	–	1.60
triglycerides	–	10.88
total lignin	36.53	36.53
C = 53.31, H = 6.41		
$\alpha = 0.5175$, $\beta = 0.8996$, $\gamma = 1$, $\delta = 0.6486$, $\epsilon = 0.9246$		
Stem wood, Cycle 2	daf	daf

cellulose	39.31	39.91
hemicellulose	24.84	25.42
lignin-c	–	0.89
lignin-h	–	26.20
lignin-o	–	3.20
tannins	–	0.01
triglycerides	–	4.37
total lignin	30.29	30.29

C = 50.94, H = 6.39
$\alpha = 0.5613$, $\beta = 0.981$, $\gamma = 0.7683$, $\delta = 0.9263$, $\epsilon = 0.9958$

Bark, Cycle 3	daf	daf
cellulose	33.78	31.38
hemicellulose	25.24	22.99
lignin-c	–	35.14
lignin-h	–	0
lignin-o	–	0
tannins	–	7.15
triglycerides	–	3.34
total lignin	34.29	35.14

C = 55.69, H = 5.89
$\alpha = 0.5265$, $\beta = 0.3359$, $\gamma = 0$, $\delta = 0$, $\epsilon = 0.8527$

Needles, Cycle 4	daf	daf
cellulose	23.59	23.59
hemicellulose	17.57	17.57
lignin-c	–	0.63
lignin-h	–	5.43
lignin-o	–	37.30
tannins	–	3.00
triglycerides	–	12.48
total lignin	43.35	43.35

C = 54.71, H = 6.36
$\alpha = 0.5225$, $\beta = 0.8364$, $\gamma = 1$, $\delta = 0.5167$, $\epsilon = 0.8996$

Bark + needles, Cycle 5	daf	daf
cellulose	23.91	23.91
hemicellulose	16.82	16.82
lignin-c	–	6.94
lignin-h	–	6.74

lignin-o	–	34.53
tannins	–	2.84
triglycerides	–	8.22
total lignin	48.21	48.21

C = 54.79, H = 6.13
$\alpha = 0.5366$, $\beta = 0.7312$, $\gamma = 0.7942$, $\delta = 0.6975$, $\epsilon = 0.9169$

Residues (rep 1), Cycle 8	daf	daf
cellulose	27.44	27.45
hemicellulose	20.80	20.81
lignin-c	–	0
lignin-h	–	3.71
lignin-o	–	32.79
tannins	–	1.98
triglycerides	–	13.27
total lignin	36.49	36.50

C = 53.85, H = 6.46
$\alpha = 0.5181$, $\beta = 1$, $\gamma = 1$, $\delta = 0.365$, $\epsilon = 0.9228$

Residues:bark:needles 1:1:1, Cycle 10	daf	daf
cellulose	24.05	24.05
hemicellulose	18.62	18.62
lignin-c	–	7.27
lignin-h	–	3.93
lignin-o	–	32.08
tannins	–	3.89
triglycerides	–	10.16
total lignin	43.28	43.28

C = 54.91, H = 6.22
$\alpha = 0.5128$, $\beta = 0.6851$, $\gamma = 0.7597$, $\delta = 0.5375$, $\epsilon = 0.8866$

Residues:bark:needles 1:2:2, Cycle 11	daf	daf
cellulose	23.98	23.99
hemicellulose	17.43	17.43
lignin-c	–	10.51
lignin-h	–	3.27
lignin-o	–	31.12
tannins	–	4.59
triglycerides	–	9.10
total lignin	44.89	44.89

C = 55.25, H = 6.14
$\alpha = 0.5285$, $\beta = 0.6664$, $\gamma = 0.6661$, $\delta = 0.5255$, $\epsilon = 0.88$

Air classified (10 Hz), Cycle 12	daf	daf
cellulose	32.44	32.44
hemicellulose	24.13	24.13
lignin-c	–	4.82
lignin-h	–	13.86
lignin-o	–	16.93
tannins	–	0
triglycerides	–	7.83
total lignin	35.60	35.60

C = 52.74, H = 6.37
$\alpha = 0.5228$, $\beta = 0.7661$, $\gamma = 0.8174$, $\delta = 0.8261$, $\epsilon = 1$

Air classified (28 Hz), Cycle 13	daf	daf
cellulose	34.37	34.37
hemicellulose	25.94	25.94
lignin-c	–	3.76
lignin-h	–	18.38
lignin-o	–	13.09
tannins	–	0
triglycerides	–	4.46
total lignin	35.23	35.23

C = 51.67, H = 6.26
$\alpha = 0.5191$, $\beta = 0.8365$, $\gamma = 0.8302$, $\delta = 0.9101$, $\epsilon = 0.9996$

Whole tree (13 yr), Cycle 15	daf	daf
cellulose	34.12	34.13
hemicellulose	25.50	25.50
lignin-c	–	0.91
lignin-h	–	16.12
lignin-o	–	16.60
tannins	–	0.66
triglycerides	–	6.08
total lignin	33.63	33.63

C = 51.63, H = 6.31
$\alpha = 0.5216$, $\beta = 1$, $\gamma = 0.9175$, $\delta = 0.845$, $\epsilon = 0.9517$

Stem wood (13 yr), Cycle 16	daf	daf
cellulose	37.46	37.46
hemicellulose	26.14	26.14
lignin-c	–	1.84
lignin-h	–	24.58
lignin-o	–	6.38
tannins	–	0.01
triglycerides	–	3.59
total lignin	32.80	32.80

C = 51.07, H = 6.31
$\alpha = 0.5387$, $\beta = 0.9443$, $\gamma = 0.7995$, $\delta = 0.9372$, $\epsilon = 0.9991$

3.3 Batch reactor and CSTR models

The material balance for a chemical reactor considers the inlet and outlet flows of the system along with accumulation and reaction effects

$$\begin{aligned} accumulation &= input - output + reaction \\ \frac{dC_A}{dt}V &= vC_{A0} - vC_A + r_A V \end{aligned} \tag{12}$$

where A represents a chemical species, C_A is the outlet concentration (mol/m^3), C_{A0} is the inlet concentration (mol/m^3), V is the reactor volume (m^3), v is the volumetric flow rate (m^3/s), and r_A is the reaction rate (mol/m^{3}s). The reaction rate is determined by multiplying a forward rate constant k by the concentration in the tank. The rate constant is calculated from an Arrhenius function

$$k = A\,T^b e^{-E/RT} \tag{13}$$

where A is the pre-exponential factor, T is the reaction temperature, b is the temperature exponent, E is the activation energy, and R is the universal gas constant.

A batch reactor was modeled to understand the time scales associated with the biomass pyrolysis kinetics. For a batch reactor, input and output is zero therefore only the accumulation and reaction terms remain in the material balance. For a constant volume reactor the V terms cancel out resulting in the following material balance for a batch reactor model

$$\begin{aligned} accumulation &= 0 - 0 + reaction \\ \frac{dC_A}{dt} &= r_A \end{aligned} \tag{14}$$

A depiction of a batch reactor can be seen in Figure 9. The Cantera Python package was used to model the batch reactor as an IdealGasReactor [5].

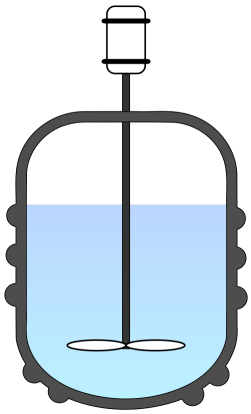

Figure 9: Representation of a batch reactor system. Source: Wikipedia.

To account for inlet and outlet flows, a continuous stirred tank reactor (CSTR) system at steady-state conditions was also modeled. The material balance for a steady-state CSTR does not account for accumulation but does consider the residence time in the system

$$\begin{aligned} 0 &= input - output + reaction \\ 0 &= vC_{A0} - vC_A + r_A V \\ C_A &= C_{A0} + r_A\,\tau \end{aligned} \tag{15}$$

where τ is the residence time (s) of chemical A in the reactor. A depiction of a CSTR system with its inlet and outlet flows is shown in Figure 10. The Cantera Python package was used to model the CSTR using an IdealGasReactor with inlet and outlet flows [5].

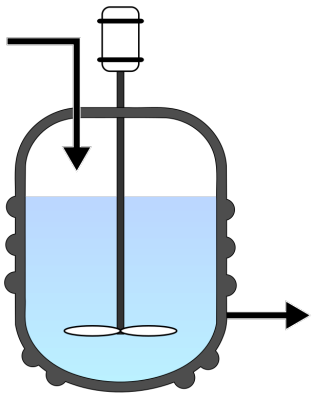

Figure 10: Representation of a continuous stirred-tank reactor (CSTR) system with inlet and outlet flows. Source: Wikipedia.

A series of continuous stirred-tank reactor (CSTR) models were used to represent the mixing (residence time) of the different feedstocks in the NREL fluidized bed reactor.

4 Results and discussion

Here.

5 Conclusions

Here.

6 Hardware requirements

The reduced order models discussed in this report were developed and executed on a MacBook Pro laptop (see hardware specs below). The models do not give as much detail as full 3D simulations but they provide good enough results in a timely manner; as such, they lend themselves well to process modeling, design of experiments, and rapid prototyping tasks.

- MacBook Pro, 16-inch, 2019 model
- 2.3 GHz 8-core Intel i9 CPU
- 32 GB 2667 MHz DDR4 memory
- 4 GB AMD Radeon Pro 5500M GPU
- macOS Big Sur version 11.6

7 Source code

Source code for this project is available on GitHub at the link provided below. See the README markdown document in the repository for more information.

- `https://github.com/wigging/fcic-pyrolysis`

References

[1] ASTM D3180-15. *Standard Practice for Calculating Coal and Coke Analyses from As-Determined to Different Bases*. West Conshohocken, PA: ASTM International, 2015.

[2] P. Debiagi et al. "A predictive model of biochar formation and characterization". In: *Journal of Analytical and Applied Pyrolysis* 134 (2018), pp. 326–335.

[3] Paulo Eduardo Amaral Debiagi et al. "Extractives Extend the Applicability of Multi-step Kinetic Scheme of Biomass Pyrolysis". In: *Energy & Fuels* 29.10 (2015), pp. 6544–6555.

[4] Richard French and Kristiina Iisa. *Personal discussions and email correspondence*. NREL, Apr. 2019.

[5] David G. Goodwin et al. *Cantera: An Object-oriented Software Toolkit for Chemical Kinetics, Thermodynamics, and Transport Processes*. Version 2.4.0. Aug. 2018. DOI: 10.5281/zenodo.1174508. URL: https://doi.org/10.5281/zenodo.1174508.

[6] William A. Rogers. Email correspondence. National Energy Technology Laboratory, May 2021.